Supporting information

Development of pH-independent Naphthalene Monoimide-based Fluorescent Probe for Hg²⁺ Detection Inside Lysosome

Rupam Roy [1], Tanoy Dutta [1], Shruti Nema [1] and Apurba Lal Koner[1*]

[1] Bionanotechnology Lab, Department of Chemistry Indian Institute of Science Education and Research Bhopal, Bhopal Bypass Road, Bhauri, Bhopal, Madhya Pradesh, India.

E-mail: akoner@iiserb.ac.in

Table of Contents

Serial No.	Content	Page No
1.	^{1}H, ^{13}C NMR and HR-MS characterizations	3-6
2.	Spectroscopic data of His-NMI-Bu	7-9
3.	DFT calculation	9-15
4.	Job's plot and fitting for binding constant	15-16
5.	Evidence for probe-metal complexation:	16-18
6.	Bioimaging studies	19-20

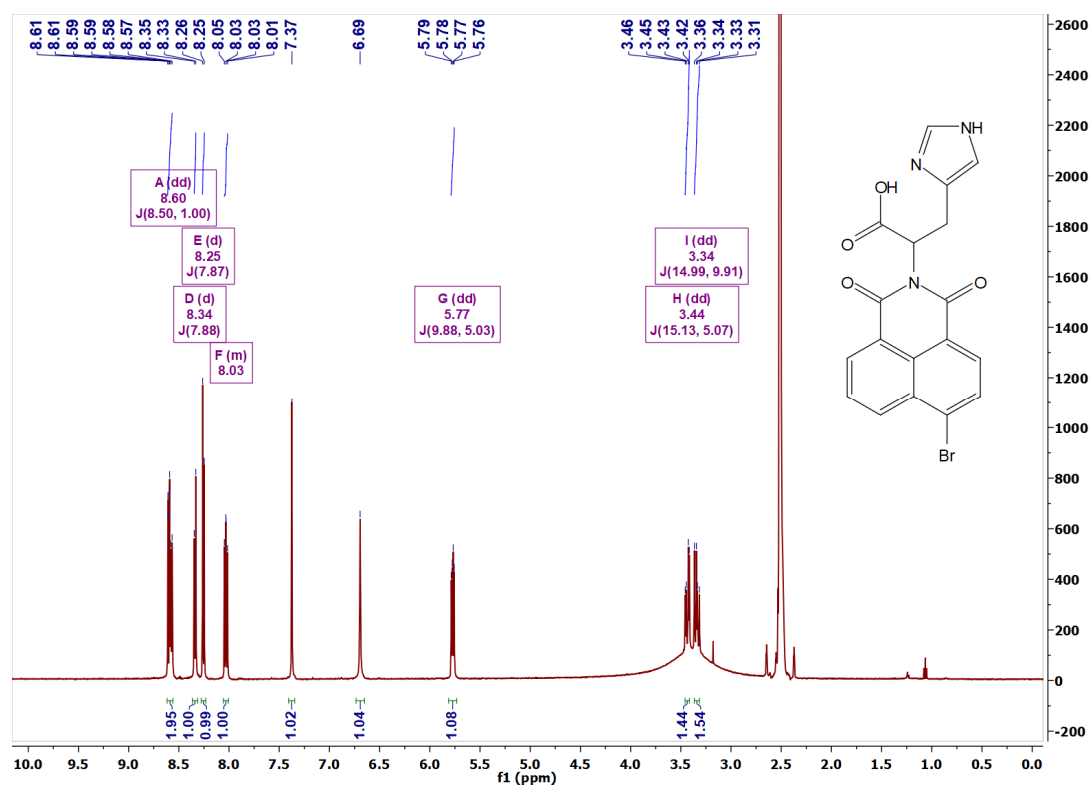## 1. ¹H, ¹³C NMR and HR-MS characterizations:

Figure S1. ¹H NMR spectrum of **His-NMI-Br** in DMSO-d_6 recorded at 500 MHz.

Note: Broadening of peaks nearby 3.25 ppm is due to overlapping of the corresponding peaks with H_2O peaks.
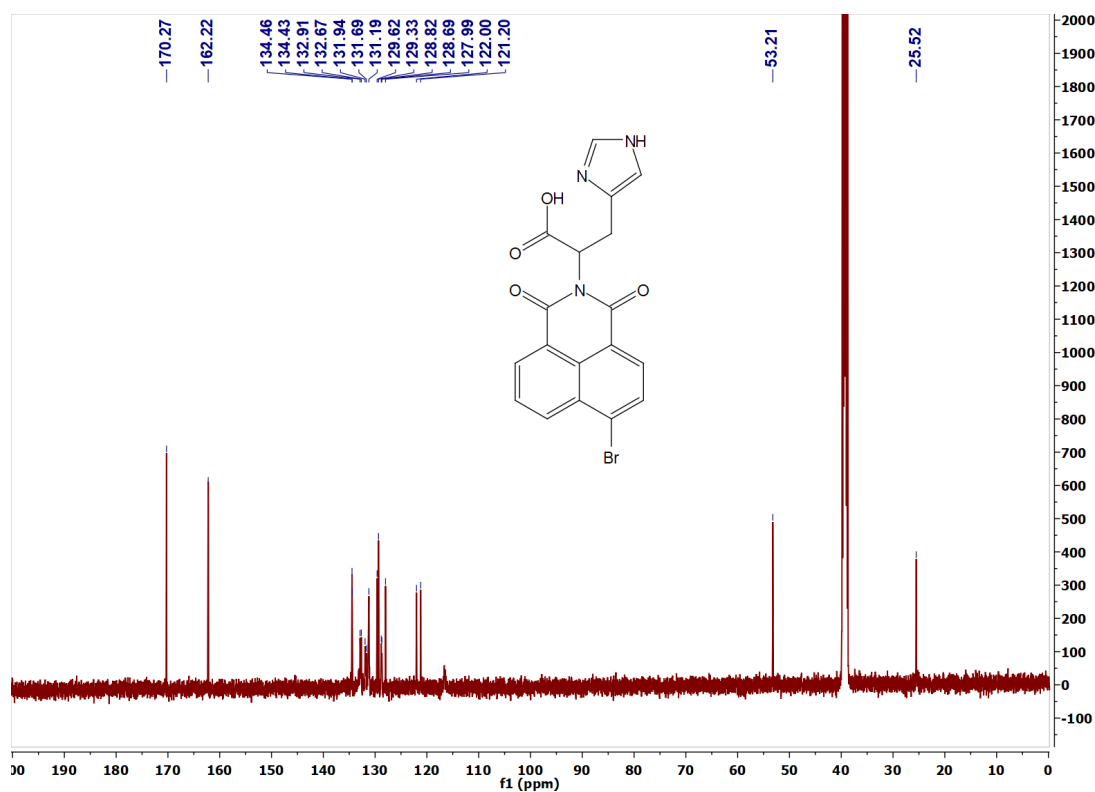

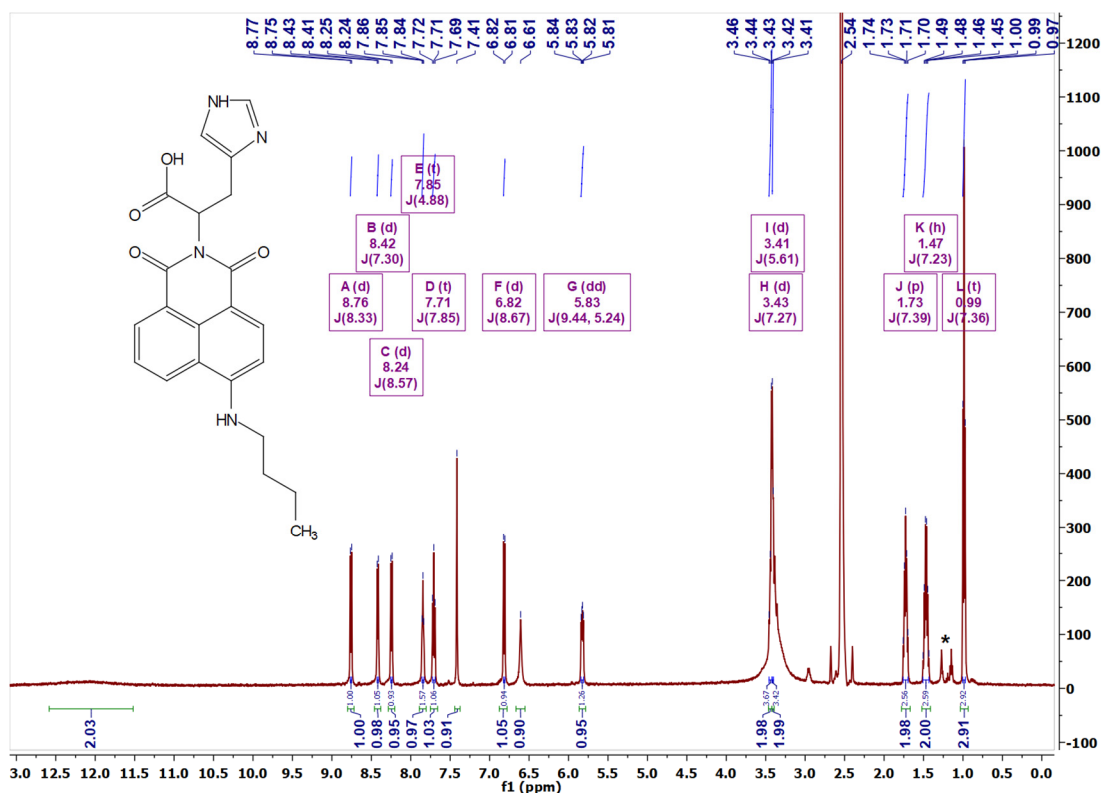**Figure S2.** ¹³C NMR spectrum of **His-NMI-Br** in DMSO-d_6 recorded at 126 MHz.

3

Figure S3. ^{1}H NMR spectrum of **His-NMI-Bu** in DMSO-d$_6$ recorded at 500 MHz. * Indicates the grease peak
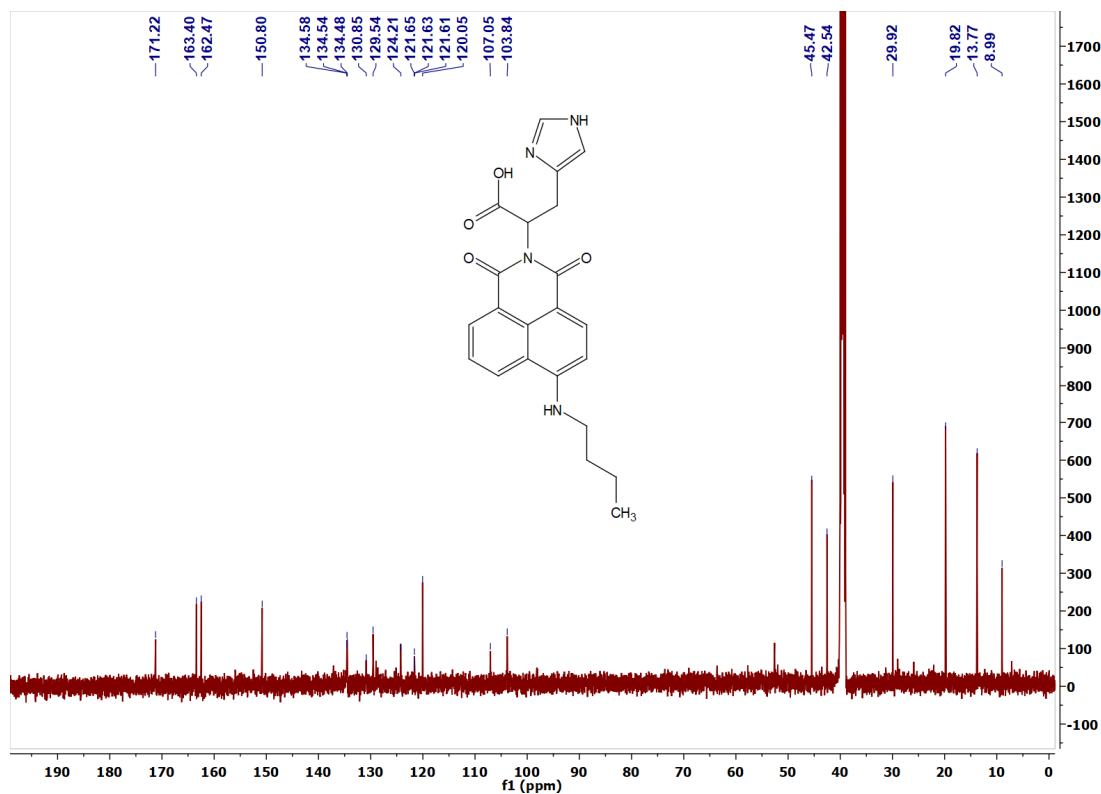

Figure S4. ^{13}C NMR spectrum of **His-NMI-Bu** in DMSO-d$_6$ recorded at 126 MHz.

Note: *In ^{1}H NMR, peak at 2.54 ppm is corresponding to residual solvent peak of DMSO.*

Acquisition Parameter
Source Type   ESI   Ion Polarity   Positive   Set Nebulizer   0.4 Bar
Focus   Not active   Set Capillary   4600 V   Set Dry Heater   180 °C
Scan Begin   50 m/z   Set End Plate Offset   -500 V   Set Dry Gas   4.0 l/min
Scan End   3000 m/z   Set Collision Cell RF   600.0 Vpp   Set Divert Valve Waste
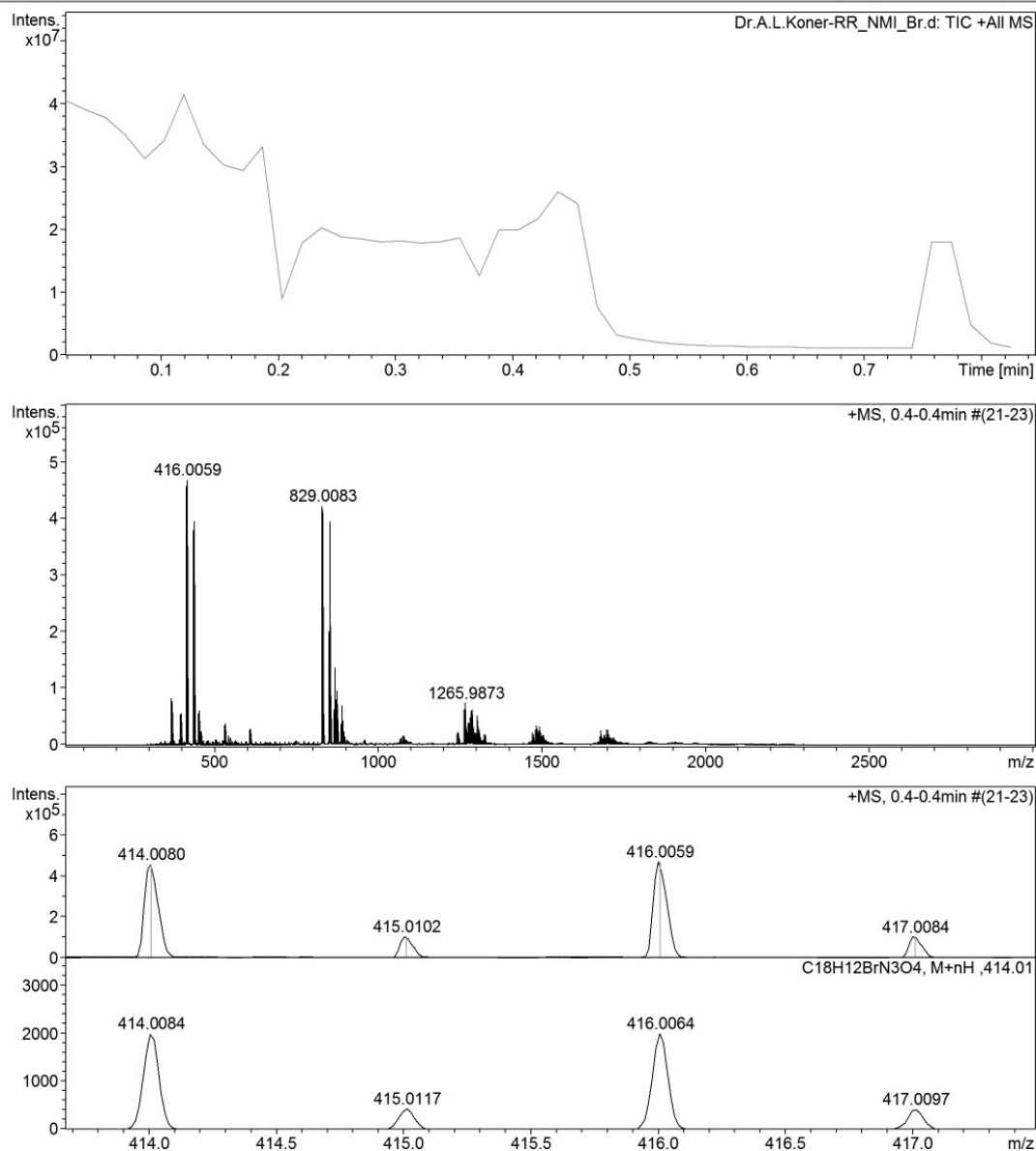
Figure S5. ESI mass spectrum of **His-NMI-Br**; **calculated mass** – 414.0089 Da, 416.0069 Da and **obtained mass** – 414.0080 Da, 416.0059 Da [M + H]⁺. Here, two molecular ion peaks with almost equal intensity and m/z difference of 2.0 Da indicate presence of Br atom in the compound. The peak at 829.0087 Da is corresponding to dimer species of **His-NMI-Br**.

$$\text{ppm error} = \frac{Calculated\ mass - Obtained\ mass}{Calculated\ mass} \times 10^6$$

$$= 2.17$$

Acquisition Parameter
Source Type   APCI   Ion Polarity   Positive   Set Nebulizer   0.4 Bar
Focus   Not active   Set Capillary   4000 V   Set Dry Heater   200 °C
Scan Begin   50 m/z   Set End Plate Offset   -500 V   Set Dry Gas   4.0 l/min
Scan End   3000 m/z   Set Collision Cell RF   600.0 Vpp   Set Divert Valve   Waste
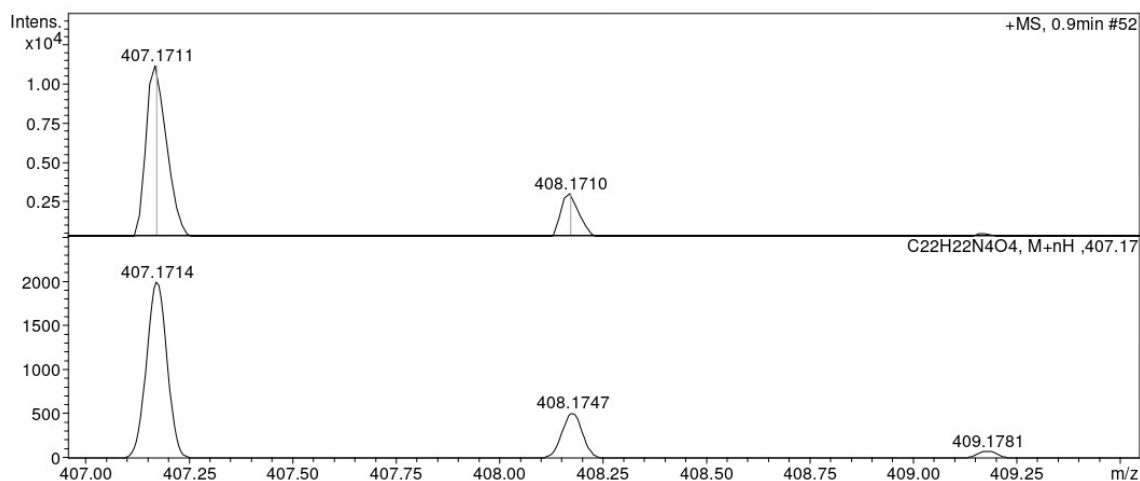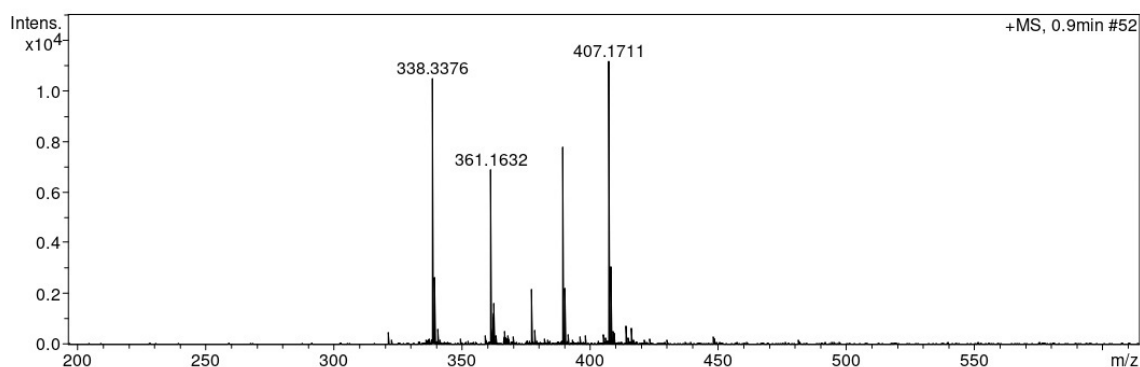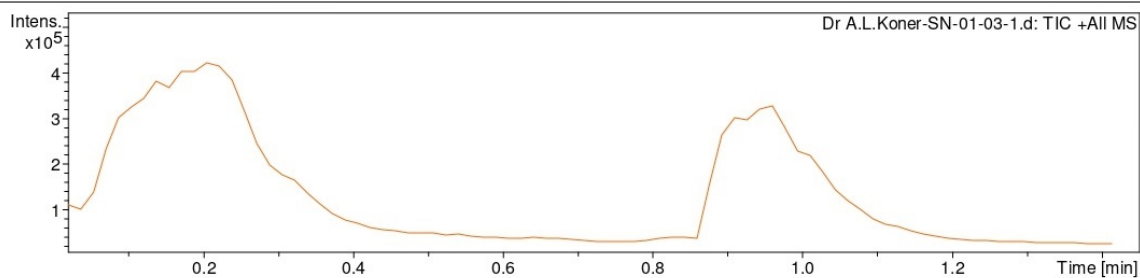
Figure S6. APCI mass spectrum of **His-NMI-Bu**; **Calculated mass** – 407.1719 Da and **obtained mass** – 407.1711 Da [M + H]$^+$.

$$\text{ppm error} = \frac{Calculated\ mass - Obtained\ mass}{Calculated\ mass} \times 10^6$$

$$= 1.96$$

6

2. Spectroscopic data of His-NMI-Bu:
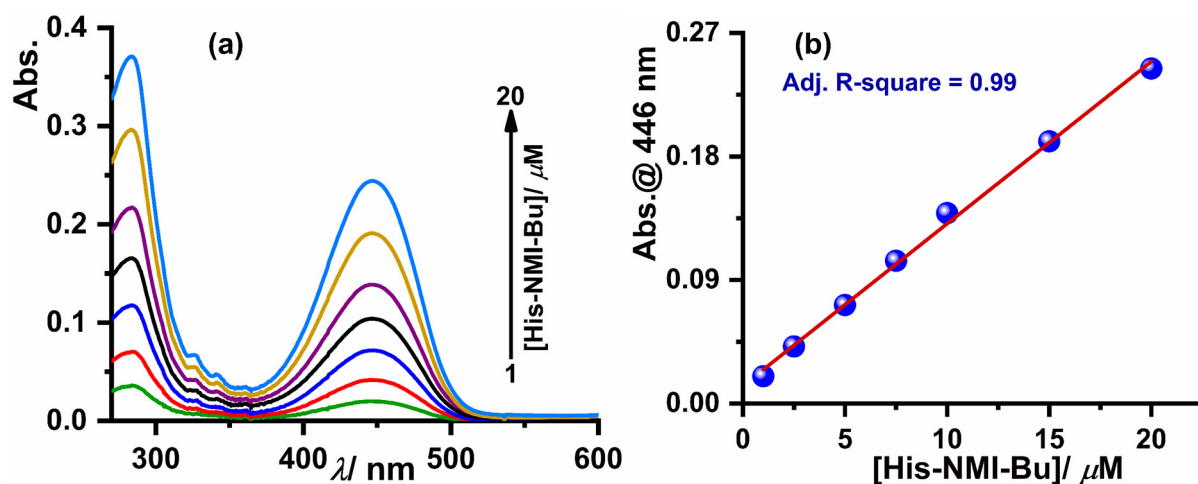

Figure S7. (a) UV-Vis. absorption spectra of probe **His-NMI-Bu** as a function of concentration in DMSO (b) Plot for absorbance at 446 nm *vs* concentration of **His-NMI-Bu** in DMSO.
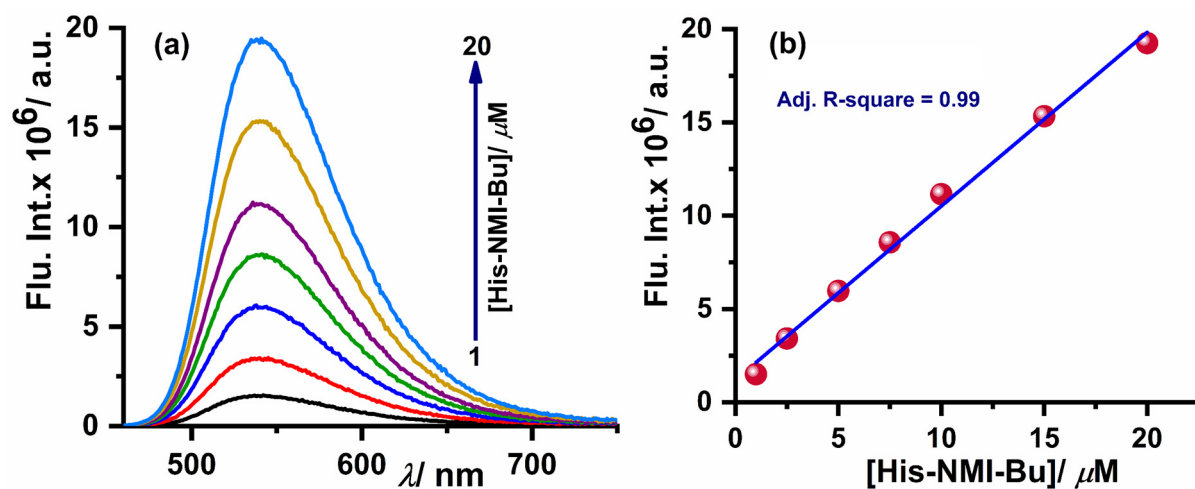

Figure S8. (a) Fluorescence spectra of probe **His-NMI-Bu** as a function of concentration in DMSO (b) Plot for fluorescence intensity at 540 nm *vs* concentration of **His-NMI-Bu** in DMSO.

Table S1. Summarization of photophysical data of **His-NMI-Bu** measured in different solvents.

Solvent	λ_{max}^{Abs}/ nm	λ_{max}^{Em}/ nm	Stokes shift/ nm	τ_i/ ns (Cont%)	τ_{avg}/ ns	Rel. Φ_{Fl}
CHCl$_3$	435	522	87	2.4 (3%), 9.7 (97%)	9.6	0.21
THF	437	521	84	10.1 (100%)	10.1	0.67
1,4-Dioxane	430	520	90	4.9 (12%), 10.5 (88%)	10.2	1.12
EtOH	439	535	96	9.2 (100%)	9.2	0.64
DMF	440	529	89	10.2 (100%)	10.2	0.69
ACN	438	534	96	10.1 (100%)	10.1	0.59
DMSO	449	539	90	10.3 (100%)	10.3	0.81
H$_2$O	455	562	107	3.4 (40%), 4.3 (60%)	4.0	0.23

Note: Relative fluorescence QY of the probe is determined using Fluoresceine as reference dye in aq. NaOH (Φ_{Fl} = 0.95 in 0.1 N NaOH)

Table S2. Radiative and non-radiative decay rates for probe in two solvents.

Solvent	$k_r \times 10^8$ (s^{-1})	$k_{nr} \times 10^8$ (s^{-1})	k_r/ k_{nr}
1,4-Dioxane	1.1	0.1	11.0
DMSO	0.8	0.2	4.0
H$_2$O	0.5	2.0	0.25

Note: The high fluorescence QY obtained in DMSO or 1,4-dioxane is attributed to predominant radiative decay rate from S_1 state to ground state. This is evident from k_r and k_{nr} values in three selective solvents such as 1,4-Dioxane, DMSO and H$_2$O.

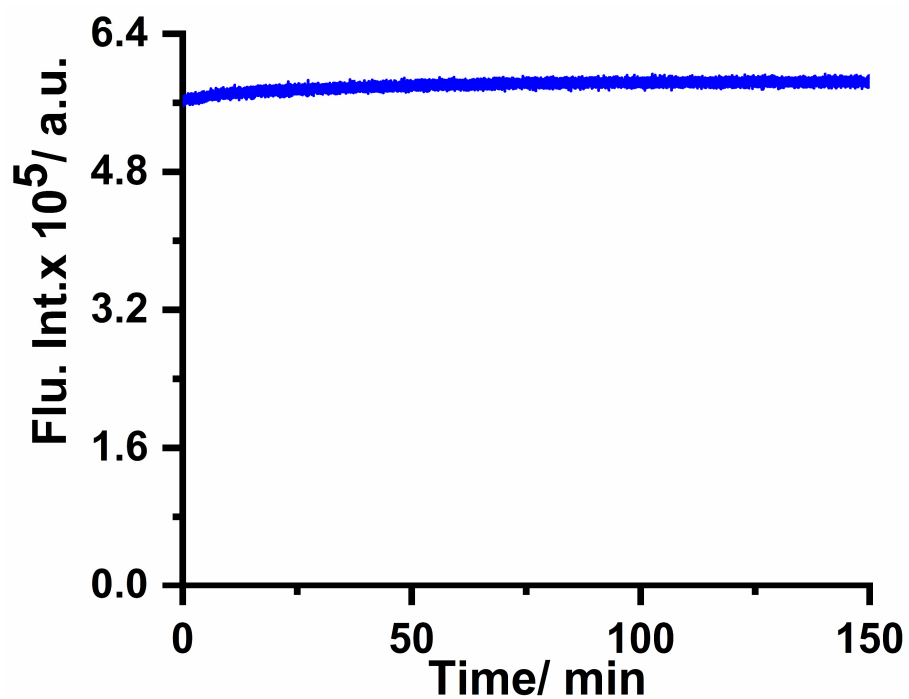**Figure S9.** Fluorescence kinetics of probe **His-NMI-Bu** (10 μM) in MES buffer (pH = 6.2) monitored at 560 nm under continuous irradiation of 450 W Xenon lamp with light intensity 100 lx.
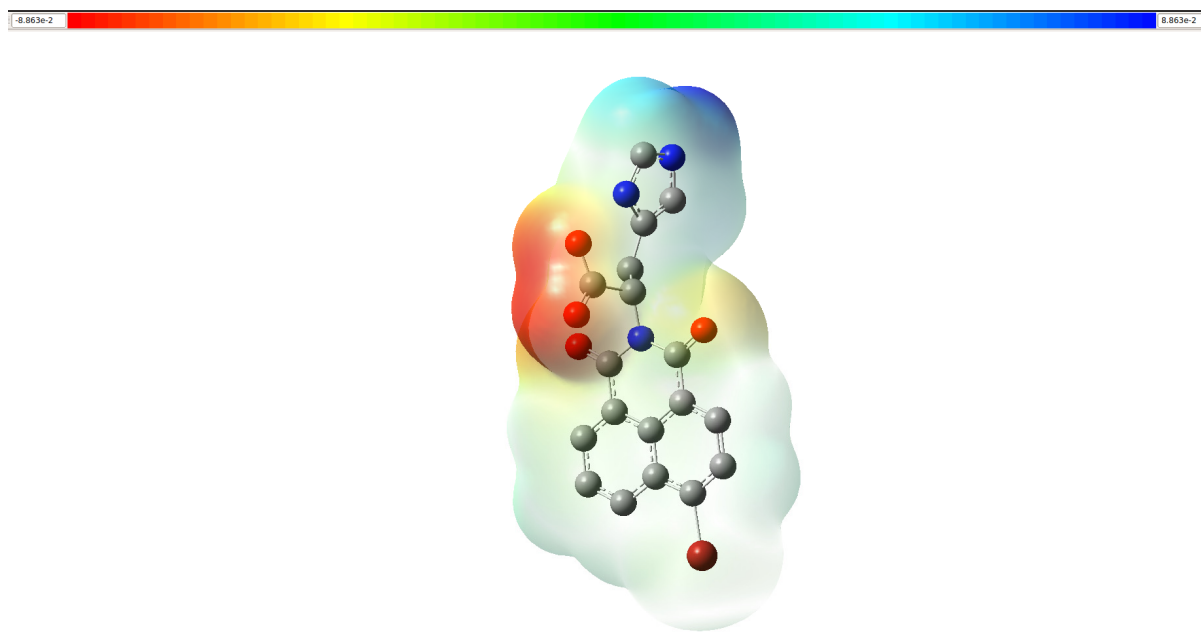
3. DFT calculation:

Figure S10. Molecular electrostatic potential map for compound **His-NMI-Br**; blue and red colors indicate positive and negative charge.

Table S3. Calculated energies of Kohn-Sham molecular orbitals (MO) of **His-NMI-Br** using DFT at the CAM-B3LYP/ LANL2DZ level of theory

FMOs	Energy/ Hartree	Energy/ eV
LUMO+5	0.04216	1.147
LUMO+4	0.03338	0.908
LUMO+3	0.02652	0.721
LUMO+2	0.00707	0.192
LUMO+1	0.00191	0.052
LUMO	-0.06449	-1.754
HOMO	-0.29536	-8.037
HOMO-1	-0.31046	-8.448
HOMO-2	-0.32193	-8.760
HOMO-3	-0.33013	-8.983
HOMO-4	-0.33660	-9.159
HOMO-5	-0.34024	-9.258

Compound: **His-NMI-Br**

Symbolic Z-matrix:
Charge = 0 Multiplicity = 1

C	-3.64217	1.69153	-0.54338
C	-3.86448	-0.75619	0.0243
C	-3.08827	0.41961	-0.21667
C	-3.27565	-1.96428	0.34395
C	-2.82401	2.78503	-0.76045
C	-0.85007	1.43745	-0.3527
C	-1.66868	0.29953	-0.11842
C	-1.07537	-0.94846	0.21152
C	-1.86679	-2.05888	0.43973
H	-1.39082	-2.99876	0.69754
C	-1.41611	2.66024	-0.66543
H	-0.76265	3.51067	-0.82888
C	0.39528	-1.07367	0.33347
C	0.62429	1.33043	-0.25605
N	1.16325	0.07622	0.08476
O	0.94575	-2.15453	0.63102
O	1.37955	2.29211	-0.4945
C	2.60739	0.00262	0.36361
H	-3.26025	3.74818	-1.00298
H	-3.88719	-2.84042	0.52526
H	-4.71875	1.79509	-0.6176
H	2.7967	-1.0451	0.61982

C	2.90104	0.82816	1.64699
O	1.98664	1.269	2.34911
O	4.19829	0.97167	1.96231
C	3.4692	0.36537	-0.87644
H	2.91597	0.0608	-1.76993
H	3.58684	1.44996	-0.93338
C	4.8051	-0.31583	-0.88202
N	5.63814	-0.25868	0.23913
C	6.75096	-0.91884	-0.05373
H	7.59292	-1.06251	0.60229
H	7.39381	-1.94682	-1.79945
N	6.68124	-1.40593	-1.33121
C	5.44896	-1.03219	-1.86743
H	5.14325	-1.29797	-2.86497
H	4.89566	0.49299	1.35945
Br	-5.80999	-0.6938	-0.08984

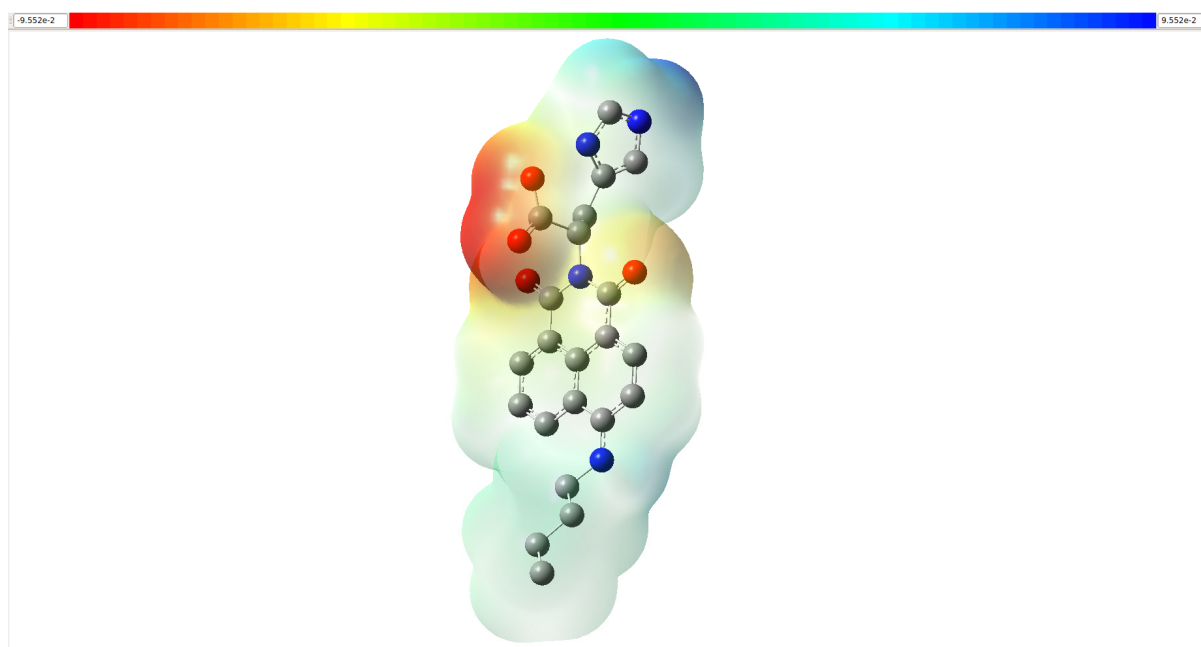**Figure S11.** Molecular electrostatic potential map for compound **His-NMI-Bu**; blue and red colors indicate positive and negative charge.

Table S4. Calculated energies of Kohn-Sham molecular orbitals (MO) of **His-NMI-Bu** using DFT at the CAM-B3LYP/ LANL2DZ level of theory.

FMOs	Energy/ Hartree	Energy/ eV
LUMO+5	0.07814	2.126
LUMO+4	0.06231	1.687
LUMO+3	0.03459	0.941

LUMO+2	0.02635	0.717
LUMO+1	0.01992	0.542
LUMO	-0.04104	-1.116
HOMO	-0.25214	-6.861
HOMO-1	-0.29914	-8.140
HOMO-2	-0.31063	-8.452
HOMO-3	-0.31490	-8.568
HOMO-4	-0.32022	-8.713
HOMO-5	-0.32187	-8.758

Compound: **His-NMI-Bu**

Symbolic Z-matrix:
Charge = 0 Multiplicity = 1

```
C          -3.11956       1.45558       -1.07655
C          -3.34745       -1.01165      -0.56
C          -2.56858       0.20061       -0.68597
C          -2.67366       -2.22386      -0.33099
C          -2.33303       2.59069       -1.1797
C          -0.37243       1.31425       -0.55893
C          -1.15748       0.13126       -0.46267
C          -0.52464       -1.1082       -0.18402
C          -1.2874        -2.27008      -0.14754
H          -0.78596       -3.21022      0.05828
C          -0.95023       2.5256        -0.89809
H          -0.31687       3.40462       -0.95542
C          0.91741        -1.18361      0.07296
C          1.08513        1.26855       -0.30405
N          1.64753        0.02295       0.00951
O          1.50716        -2.25854      0.33057
O          1.81082        2.28152       -0.39088
C          3.05474        -0.01138      0.43324
H          -2.77819       3.53241       -1.48279
H          -3.25349       -3.13946      -0.25061
H          -4.16766       1.52954       -1.32919
N          -4.72884       -1.0537       -0.67157
H          -5.11552       -1.98865      -0.72418
C          -5.70743       -0.0238       -0.29743
H          -5.25907       0.66027       0.43254
H          -6.01505       0.57252       -1.16848
C          -6.95446       -0.67457      0.31573
H          -7.37114       -1.40578      -0.394
H          -6.66757       -1.22958      1.21931
C          -8.03735       0.35783       0.66501
H          -7.62362       1.09484       1.36711
H          -8.31792       0.91206       -0.24159
C          -9.28721       -0.28992      1.27852
H          -10.04666      0.46173       1.52078
```

|			
H	-9.7377	-1.01053	0.58484
H	-9.03875	-0.82543	2.20283
H	3.26425	-1.06762	0.63441
C	3.18438	0.72858	1.79171
O	2.19189	1.07818	2.43593
O	4.44035	0.90374	2.24197
C	4.01963	0.47446	-0.68311
H	3.5681	0.22093	-1.64684
H	4.09614	1.56373	-0.64862
C	5.37647	-0.15862	-0.60643
N	6.10112	-0.1492	0.58927
C	7.25973	-0.75322	0.36074
H	8.04302	-0.91367	1.08231
H	8.09734	-1.64435	-1.37822
N	7.32582	-1.15738	-0.94598
C	6.13418	-0.78776	-1.57033
H	5.9297	-0.998	-2.60624
H	5.21079	0.4984	1.68172
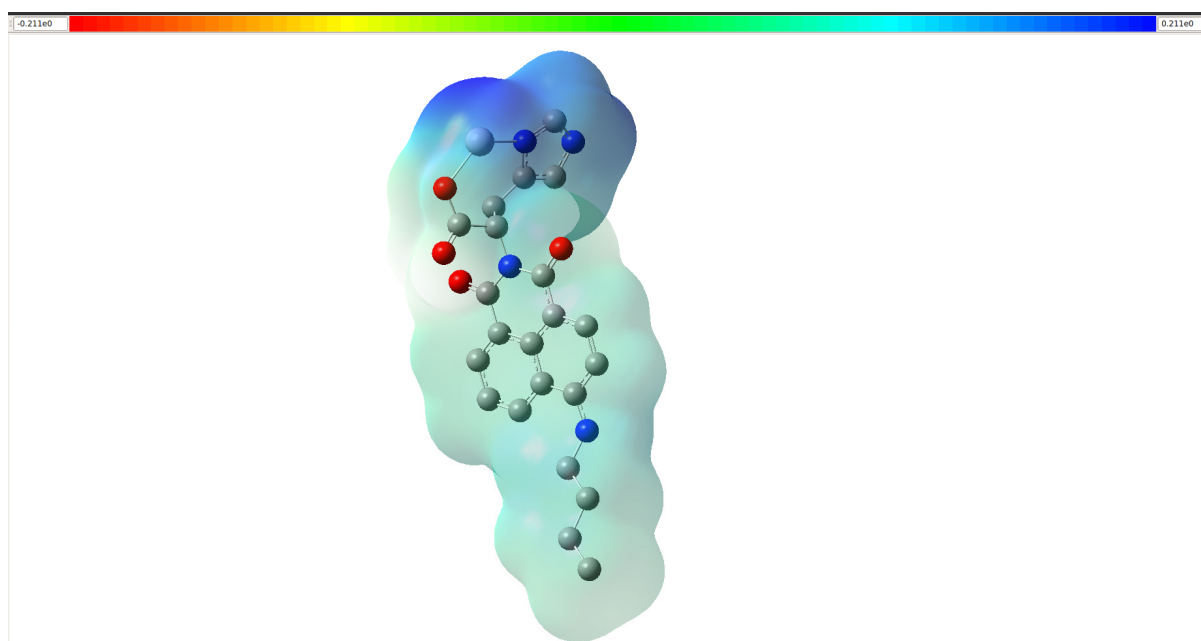
Figure S12. Molecular electrostatic potential map for compound **His-NMI-Bu** + Hg^{2+}; blue and red colors indicate positive and negative charge.

Table S5. Calculated energies of Kohn-Sham molecular orbitals (MO) of **His-NMI-Bu** + Hg^{2+} using DFT at the CAM-B3LYP/ LANL2DZ level of theory.

FMOs	Energy/ Hartree	Energy/ eV
LUMO+5	-0.06829	-1.858
LUMO+4	-0.07063	-1.921
LUMO+3	-0.10415	-2.834
LUMO+2	-0.12209	-3.322

LUMO+1	-0.13199	-3.591
LUMO	-0.23405	-6.368
HOMO	-0.32655	-8.885
HOMO-1	-0.39262	-10.683
HOMO-2	-0.40088	-10.908
HOMO-3	-0.41129	-11.191
HOMO-4	-0.41514	-11.296
HOMO-5	-0.42664	-11.609

Compound: **His-NMI-Bu + Hg²⁺**

Symbolic Z-matrix:
Charge = 1 Multiplicity = 1

C	4.75274	-0.83556	-1.44138
C	4.79405	0.95025	0.36256
C	4.09874	0.0152	-0.50565
C	4.02147	1.82718	1.16237
C	4.04976	-1.71819	-2.24797
C	1.96888	-0.95741	-1.27967
C	2.66737	-0.03501	-0.4479
C	1.94005	0.83795	0.40725
C	2.63452	1.76811	1.18658
H	2.06563	2.4317	1.82982
C	2.64718	-1.79155	-2.15735
H	2.07558	-2.48425	-2.76627
C	0.49482	0.77305	0.49648
C	0.5018	-1.04581	-1.22431
N	-0.15474	-0.19074	-0.32087
O	-0.21299	1.50676	1.2355
O	-0.18118	-1.8066	-1.94674
C	-1.58712	-0.37252	-0.11225
H	4.5823	-2.35172	-2.94829
H	4.53666	2.54033	1.79956
H	5.82418	-0.79624	-1.55629
N	6.15557	1.0646	0.4779
H	6.46132	1.82106	1.07968
C	7.24737	0.18031	0.04803
H	6.97603	-0.8664	0.23179
H	7.45108	0.29876	-1.02487
C	8.52193	0.51755	0.8312
H	8.77557	1.57731	0.67927
H	8.33856	0.37776	1.90547
C	9.71359	-0.35062	0.39825
H	9.46353	-1.41088	0.54169
H	9.89446	-0.21252	-0.67675
C	10.9919	-0.01563	1.1801
H	11.82878	-0.64431	0.85824
H	11.28328	1.03102	1.03045
H	10.84941	-0.17397	2.25582

H	-1.82634	0.41534	0.61829
C	-1.84546	-1.72104	0.61764
O	-0.95706	-2.50465	0.91955
O	-3.15199	-1.97072	0.99425
C	-2.42684	-0.14914	-1.41713
H	-1.74088	-0.14275	-2.26332
H	-3.07334	-1.01546	-1.61023
C	-3.23529	1.12094	-1.42951
N	-4.35498	1.31851	-0.58541
C	-4.86592	2.53073	-0.83713
H	-5.71946	2.98039	-0.35778
H	-4.29765	4.04271	-2.19105
N	-4.13118	3.11945	-1.80889
C	-3.1078	2.25479	-2.19357
H	-2.38779	2.50653	-2.95358
Hg	-4.52255	-0.39509	0.78973

Binding energy calculation:

$E = E_{His\text{-}NMI\text{-}Bu+Hg2+} - (E_{His\text{-}NMI\text{-}Bu} + E_{HgCl2} - 1/2E_{H2})/$ Hartree

$= -1412.477 - (-1370.669 - 72.583 + 0.587)/$ Hartree

$= -30.188$ Hartree

$= -7.9 \times 10^4$ KJ/ mol

Note: Here, E is considered as electronic energy of the optimized geometry.

4. Job's plot and fitting for binding constant:
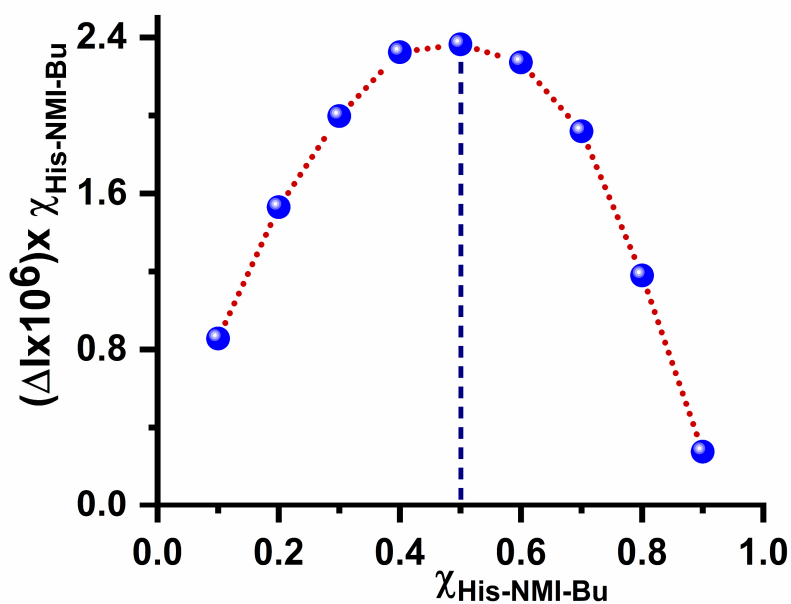
Figure S13. Job's plot for **His-NMI-Bu** with $HgCl_2$ in MES buffer at pH 6.2.
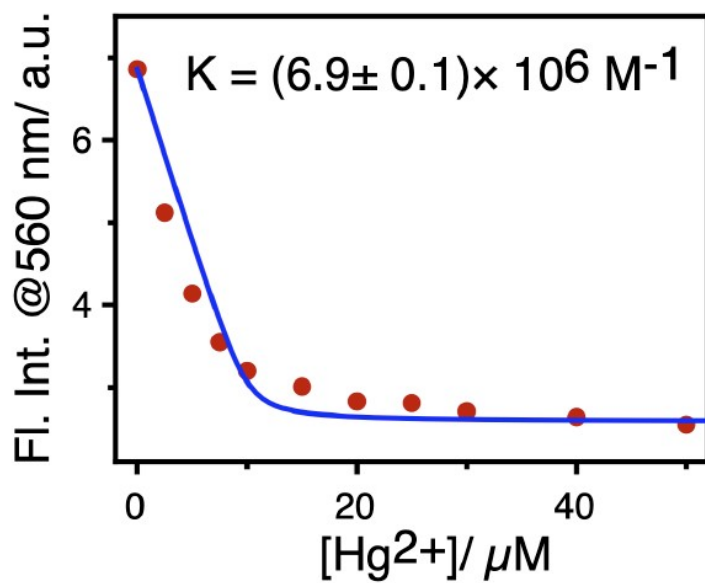
Figure S14. Fitted plot of fluorescence intensity as a function of Hg^{2+} concentration resulting the binding constant value.
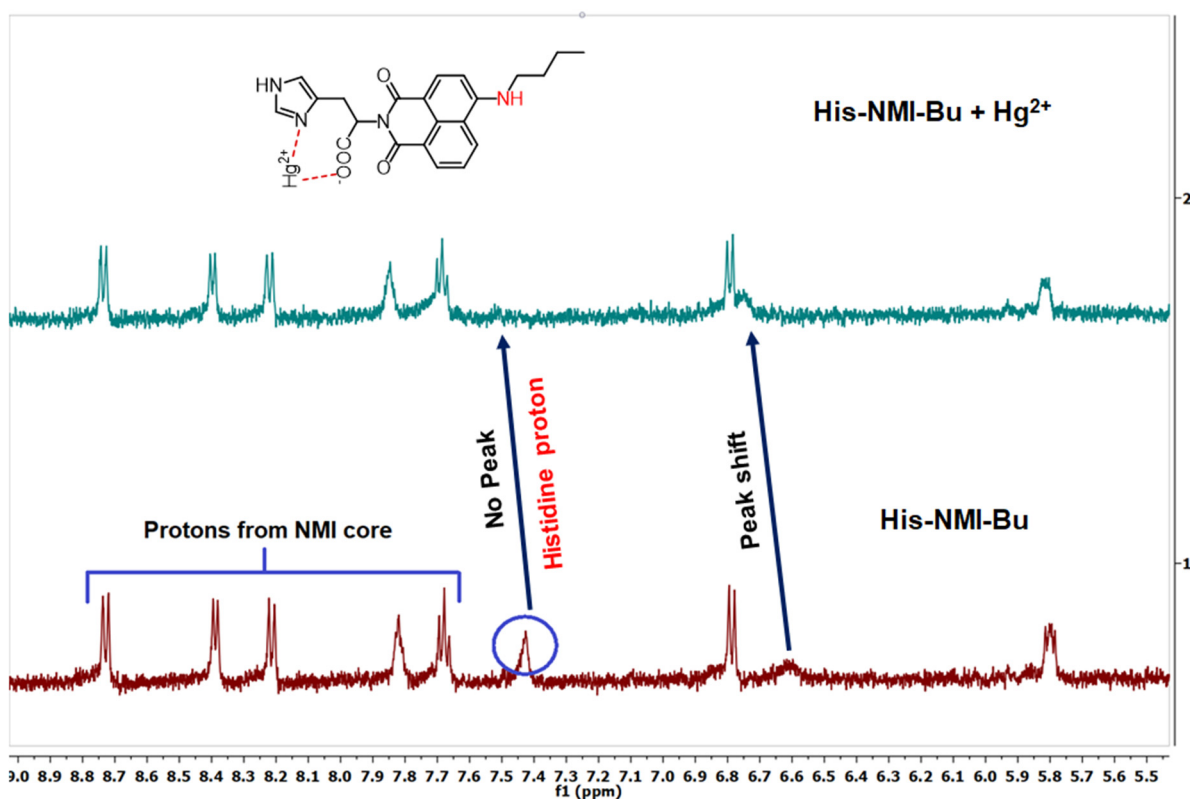
5. Evidence for probe-metal complexation:

Figure S15. Comparison of ^1H NMR spectra between only **His-NMI-Bu** (1.0 mM) and **His-NMI-Bu** + 2.0 mM $HgCl_2$ complex in DMSO-d_6 recorded at 500 MHz.

Note: ^1H NMR spectra of the probe shows appearance of peaks corresponding to NMI core in 7.6-9.0 ppm region. The peak positioned at 7.4 ppm originates from histidine moiety. After chelation of the probe with Hg^{2+}, the complex shows disappearance of 7.4 ppm peak and the peak at 6.6 ppm exhibits downfield shift with respect to probe only. The vanishing of peak occurs due to formation of charged species located on imidazole N-atom. Also, the downfield shift for 6.6 ppm peak corresponding to H_a/ H_b proton might be due to experiencing different magnetic field after formation of charged complex. This NMR titration results indicate formation of metal-probe complex via chelation which is the key complexation mechanism here.
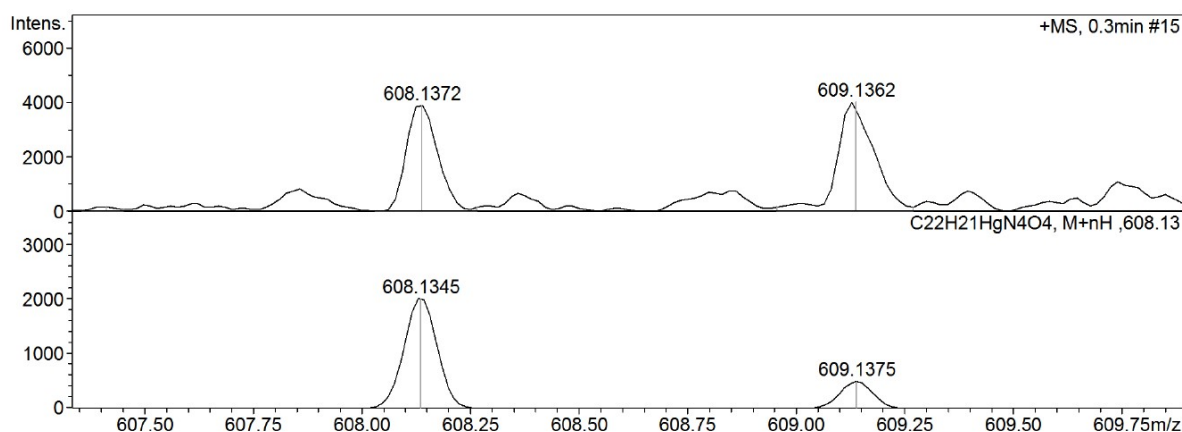
Figure S16. ESI mass spectrum of **His-NMI-Bu + Hg^{2+}** complex; **calculated mass** – 607.1264 and **obtained mass** – *m/z* 608.1372 [M + H]$^+$.
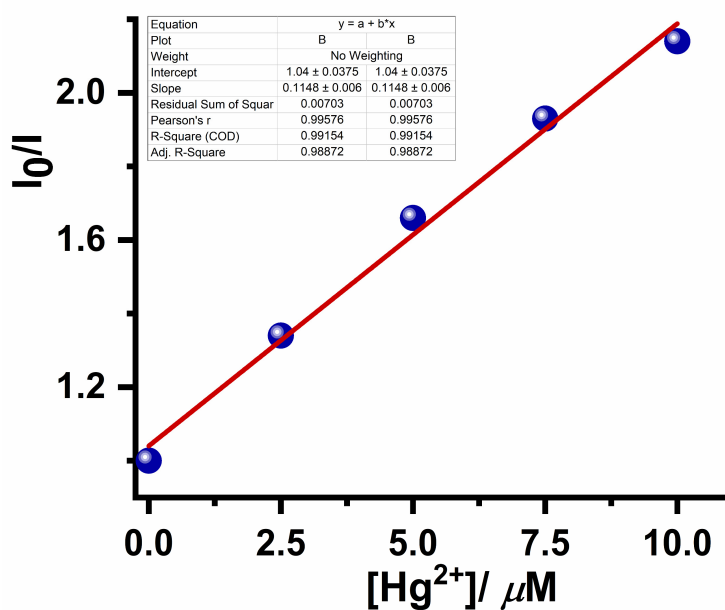

Figure S17. Plot of I_0/I *vs* concentration of Hg^{2+} derived from concentration-dependent fluorescence study in MES buffer (pH = 6.2).
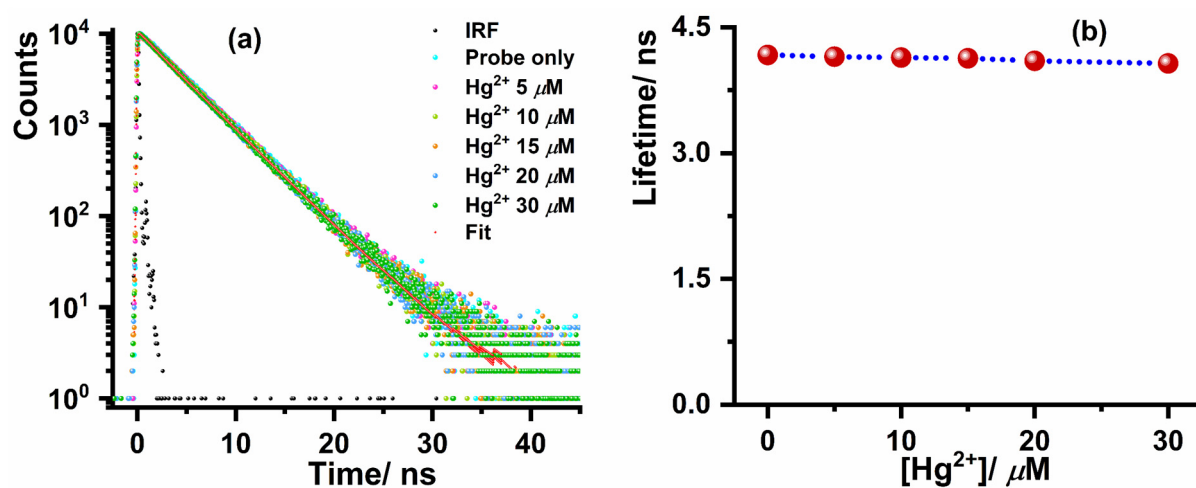
Figure S18. (a) Time-resolved fluorescence decay of **His-NMI-Bu** with $HgCl_2$ of different concentration in MES buffer (b) plot for average lifetime *vs* concentration of Hg^{2+} in MES buffer (pH = 6.2).

Table S6. Detailed fluorescence lifetime values with contribution of components in MES buffer pH 6.2.

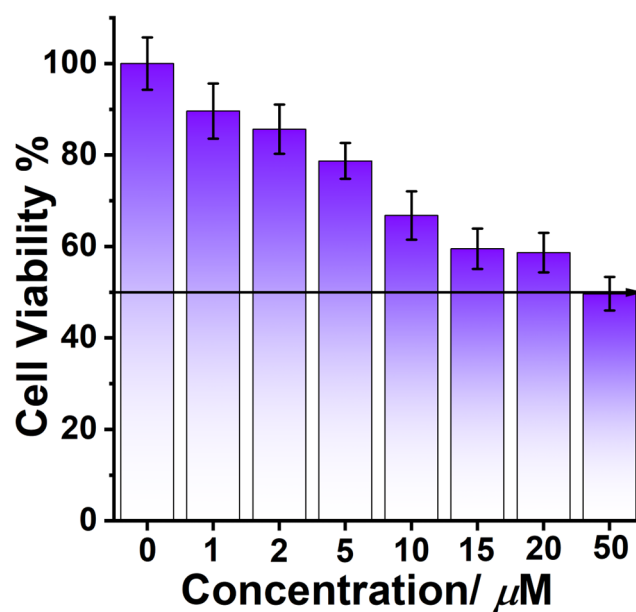| Entry	τ_1/ ns (Cont.%)	τ_2/ ns (Cont.%)	τ_{avg}/ ns
Probe	2.96 (13%)	4.30 (87%)	4.17
Probe + 5 μM Hg^{2+}	2.06 (4%)	4.20 (96%)	4.15
Probe + 10 μM Hg^{2+}	1.11 (2%)	4.15 (98%)	4.14
Probe + 15 μM Hg^{2+}	1.48 (3%)	4.16 (97%)	4.13
Probe + 20 μM Hg^{2+}	1.54 (4%)	4.14 (96%)	4.10
Probe + 30 μM Hg^{2+}	1.08 (3%)	4.10 (97%)	4.07

6. **Bioimaging studies:**

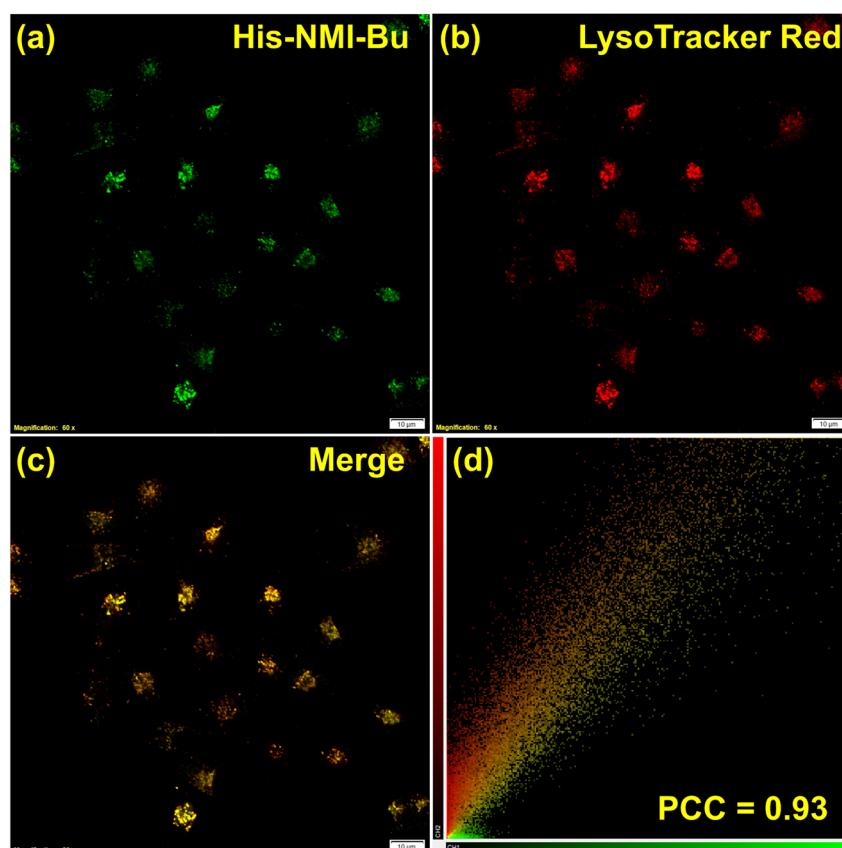**Figure S19.** MTT assay showing cell viability in the presence of probe **His–NMI–Bu** (0-50 μM).

Figure S20. Confocal live-cell colocalization experiments in Hela cells. (a) shows the FITC channel images stained with 5 μM **His-NMI-Bu**; (b) show TRITC channel images stained with 0.3 μM LysoTracker Red (c) shows the merge image of (a) and (b); (d) shows the scatter plot to get the respective Pearson's correlation coefficient.
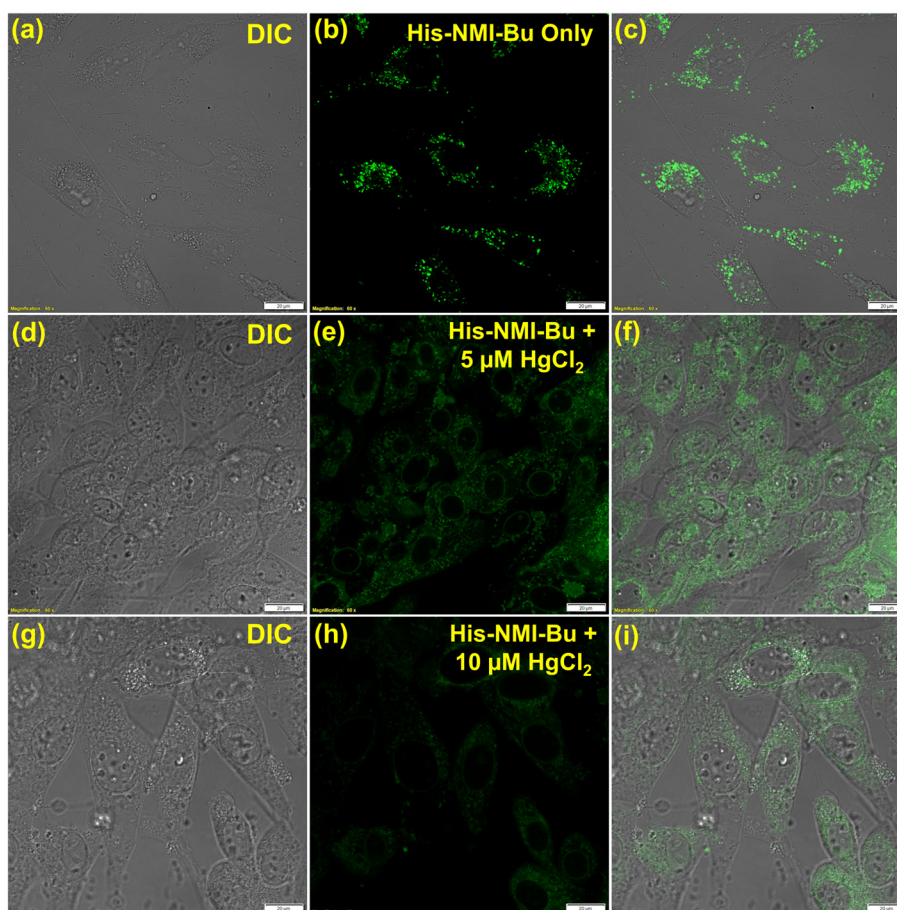
Figure S21. CLSM images of live BHK-21 cells showing the intracellular response of Hg^{2+}. (a-c) show images of cells stained with 5 μM **His-NMI-Bu** only; (d-f) show images of cells pre-incubated with 5 μM HgCl$_2$ and stained with 5 μM **His-NMI-Bu**; (g-i) show images of cells pre-incubated with 10 μM HgCl$_2$ and stained with 5 μM **His-NMI-Bu**. The gradual decrease in fluorescence intensity confirms the detection of Hg^{2+} inside lysosomal compartment.